







Article

Photo-Activated Carbon Dots as Catalysts in Knoevenagel Condensation: An Advance in the Synthetic Field

Cinzia Michenzi ¹, Francesca Scaramuzzo ¹, Chiara Salvitti ², Federico Pepi ², Anna Troiani ^{2,*}
and Isabella Chiarotto ^{1,*}

¹ Department of Basic and Applied Sciences for Engineering, Sapienza University of Rome, Via Castro Laurenziano 7, 00161 Roma, Italy; cinzia.michenzi@uniroma1.it (C.M.); francesca.scaramuzzo@uniroma1.it (F.S.)

² Department of Chemistry and Technology of Drugs, Sapienza University of Rome, P.le Aldo Moro 5, 00185 Roma, Italy; chiara.salvitti@uniroma1.it (C.S.); federico.pepi@uniroma1.it (F.P.)

* Correspondence: anna.troiani@uniroma1.it (A.T.); isabella.chiarotto@uniroma1.it (I.C.)

Abstract: Photoinduced chemical reactions and the development of new materials represent a current and significant topic. We present a sustainable and eco-friendly approach to the Knoevenagel condensation reaction involving carbonyl and active methylene compounds. Our method utilizes photo-activated carbon dots (CDs) derived from 5-hydroxymethylfurfural (5HMF) within an aqueous medium and does not require acidic, basic, or thermal conditions. This protocol operates effectively with aromatic, aliphatic, and heteroaromatic aldehydes and ketones. The 5HMF-derived-CDs can be reused four times without significant loss of activity. Moreover, this methodology is suitable for scaling up reactions, thereby highlighting its potential for industrial applications.

Keywords: carbon dots; Knoevenagel condensation; photochemistry; 5-hydroxymethylfurfural; scale-up synthesis



Citation: Michenzi, C.; Scaramuzzo, F.; Salvitti, C.; Pepi, F.; Troiani, A.; Chiarotto, I. Photo-Activated Carbon Dots as Catalysts in Knoevenagel Condensation: An Advance in the Synthetic Field. *Photochem* **2024**, *4*, 361–376. <https://doi.org/10.3390/photochem4030022>

Academic Editor: Yasuharu Yoshimi

Received: 16 July 2024

Revised: 6 August 2024

Accepted: 20 August 2024

Published: 27 August 2024



Copyright: © 2024 by the authors. Licensee MDPI, Basel, Switzerland. This article is an open access article distributed under the terms and conditions of the Creative Commons Attribution (CC BY) license (<https://creativecommons.org/licenses/by/4.0/>).

1. Introduction

Modern chemical research must improve the processes of sustainable and environmentally friendly chemistry. Sustainable chemistry aims to enhance the efficiency of utilizing natural resources for chemical products [1]. This involves identifying ways to reduce energy consumption employing environmentally benign chemicals and effectively managing material end-of-life [2]. Over the past two decades, a unique class of carbon nanomaterials has garnered considerable interest among scientists, particularly in the fields of nanomaterial science and biomass conversion: carbon dots (CDs). These nanomaterials epitomize an innovative category of nanoparticles with a wide range of applications [3]. Their interest stems from their fluorescence properties, chemical stability, minimal toxicity, environmental friendliness, affordability, and strong biocompatibility [4]. Their unique properties enable CDs to find applications in various fields, including biomedicine, catalysis, and chemical sensing for a wide range of analytes, such as cations, anions, and small molecules [5].

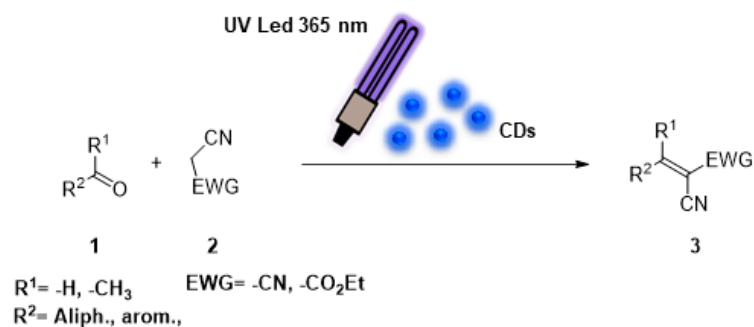
There is considerable interest in synthetic methods that enable CD production from biomass or renewable natural resources, including plants, vegetables, fruits, beverages, juices, or organic waste in general [6]. Their production from biomass or biomass derivatives allows the requalification of the biowastes by converting raw materials into value-added products [7–9]. 5-Hydroxymethylfurfural (5HMF) emerges as a pivotal platform chemical, finding widespread application across various industries. It represents a key component in the array of products derived from biomass [10]. The existence of 5HMF in agricultural food waste following the thermal treatment of sugar-containing foods and beverages [11] gives the opportunity to utilize biowastes to obtain carbon nanomaterials through an electrochemical oxidative process. In the area of the production of carbon nanomaterials from small molecules, the use of the electrochemical method represents a

particularly innovative method [12]. Thanks to their unique characteristics and optical properties, CDs have paved the way for their utilization as nano-organocatalysts [13,14] and photocatalysts [15,16]. In the continued interest of protecting the environment and continued progress in green chemistry and sustainability, the study of renewable energy sources for the development of eco-friendly systems has led to considerable attention on efficient and selective chemical transformations. In this context, photocatalysis emerges as a compelling field within green chemistry, as it seamlessly integrates the benefits of catalysis with the utilization of renewable energy sources [17]. Photochemistry has been studied for many years and can represent a valid alternative to offer safer, more economical, environmentally friendly, sustainable, and greener solutions [18]. CD-based materials, an emerging class of low-cost photocatalysts, have undergone extensive investigation for their role in photoinduced cleavage and the formation of carbonous chemical bonds [19]. Moreover, CDs can also behave as both electron donors and electron acceptors when photoexcited by UV-vis light, thus enabling the synthesis of important organic compounds through light-driven radical mechanisms [20]. Light radiation is indeed a non-hazardous and eco-friendly source of energy [21]. The Knoevenagel condensation reaction finds extensive use in the field of organic synthesis and several reaction conditions have been applied. Among the processes for forming carbon-carbon bonds, Knoevenagel condensation stands out as a variation of the traditional aldol condensation. It involves the reaction between an active methylene compound and a carbonyl compound (either an aldehyde or a ketone), followed by the elimination of a water molecule [22]. Products obtained are extensively used in many applications, such as natural products, functional polymers [23,24], flavors, and perfumes [25], or intermediates such as carbocyclic, substituted alkenes [26,27]. The most recent applications of Knoevenagel condensation products across diverse industries have facilitated the total synthesis of therapeutic drugs serving as anticancer agents [28]. Additionally, they have enabled the production of symmetric dibenzylideneacetones, which exhibit valuable biological and industrial properties, including antibacterial effects and potential UV filter activity [29].

The most widely accepted mechanism involves the deprotonation of the active methylene substrate by a base, followed by nucleophilic addition to the carbonyl group of the aldehyde (or ketone) [30,31]. To this end, mass spectrometric techniques, specifically employed for the isolation and characterization of transient species [32–34], revealed the intervention of different reaction intermediates depending on the catalytic system chosen [35]. CDs were successfully used in Knoevenagel condensation as organo- [13] or as heterogeneous photocatalysts under different reaction conditions [36]. Significant reductions in reaction times are attainable through the utilization of CD catalysts under UV irradiation. However, to the best of our knowledge, the activity of carbon materials under photocatalytic conditions and the related mechanism in the Knoevenagel reaction have been poorly investigated [37,38]. To this purpose, a preliminary mass spectrometric study contributed to highlighting the key role of UV light in the photo-activation of CD catalysts, postulating a possible aldol-mediated mechanism for the formation of the condensation product [39]. Specifically, irradiation of hydroxyl-functionalized CDs with light can amplify the hydrogen bonding between the surface OH groups of the CDs and the electrophilic carbonyl group, thereby facilitating aldol condensation [40,41]. Therefore, the catalytic mechanism and resulting reaction outcome are contingent upon the luminescence of CDs and their surface properties. Here, an effective synthetic protocol for the Knoevenagel condensation photocatalyzed by CDs was developed, and its potential scalability for large-scale applications was verified. The presented procedure is suitable with both electron donation and electron withdrawal substituents present on aromatic, aliphatic or heteroaromatic aldehydes, and ketones. The reaction was studied with the ethyl cyanoacetate and malononitrile even if it is equally applicable to other active methylene compounds.

2. Results and Discussion

In our present study, the use of CDs for the photochemical Knoevenagel reaction is reported (Scheme 1).



Scheme 1. Photo-activated carbon dots as catalysts in Knoevenagel condensation. EWG as Electron-withdrawing group.

5HMF derived-CDs (denoted as HMF-CDs) were employed as photocatalysts for C–C bond formation in organic synthesis. HMF-CDs exhibited promising photo-enhanced catalytic performance, yielding 93% in 30 min when 4-fluorobenzaldehyde and ethyl cyanoacetate (*vide infra*) were utilized in the Knoevenagel condensation reaction. A series of catalytic experiments substantiated that the catalytic efficacy of HMF-CDs can be significantly augmented by light, likely owing to the involvement of active species in the photocatalytic mechanism of HMF-CDs. The effectiveness of HMF-CDs in photocatalyzing Knoevenagel condensation was ascertained with respect to different light sources to achieve the optimized photoreaction conditions. HMF-CDs were prepared via alkaline-assisted electrochemical *bottom-up* synthesis, and their characterizations (SEM, TEM, EDX, XRD, PL, FTIR, DLS-Zero Potential, and TGA) have revealed interesting chemical-physical properties that have suggested use of the synthesized HMF-CDs as catalysts [14] and, in this work, as photocatalysts. The UV-Vis absorption spectrum of the HMF-CDs showed a band at approximately 250 nm (Figure S1). However, from an application point of view, the strong PL emission intensity of nanoparticles remains one of the most common features of CDs. Fluorescence spectra (PL) were examined to probe the optical properties of HMF-CDs. In Figure 1, the nanoparticles synthesized via the electrochemical *bottom-up* technique exhibited strong fluorescence when illuminated with UV light ($\lambda_{\text{max exc.}} = 370 \text{ nm}$).

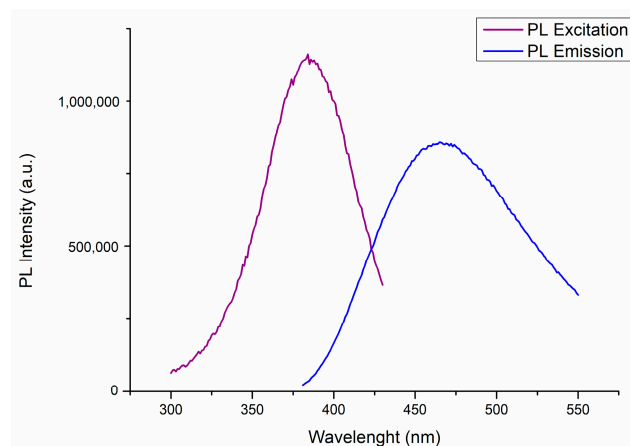


Figure 1. Optical properties of HMF-CD PL spectra.

A comparable photoluminescent characteristic of HMF-CDs has been documented in the literature and attributed to factors such as nanomaterial size, presence of sp^2 sites, aromatic conjugate structure, and structural defects [42]. Our preliminary investigation

for photocatalytic Knoevenagel condensation was begun with a model reaction between *p*-anisaldehyde (**1a**) as electrophile and malononitrile (**2a**) or ethyl cyanoacetate (**2b**) as nucleophiles in the presence of 10 mg of HMF-CDs as agents for absorbing light. In accordance with sustainable development goals and the green chemistry imperative, water and ethanol were chosen as the polar green solvents for the reaction. All the reactions were conducted at room temperature, and it was found that a catalyst loading of 10 mg was most effective. The results obtained are summarized in Table 1.

Table 1. Investigation of the reaction conditions for the synthesis of products **3aa/3ab**^a.

Reaction scheme: *p*-anisaldehyde (**1a**) + nucleophile (**2a** or **2b**) $\xrightarrow[\text{solvent, r.t, light source}]{\text{HMF-CDs}}$ product (**3aa** or **3ab**)

1a: COc1ccc(C=O)cc1
2a Y = CN
2b Y = CO₂Et
3aa COc1ccc(C=C(C#N)Y)cc1
3ab COc1ccc(C=C(C#N)Y)cc1

Entry	Catalyst Loading (mg)	2	Solvent	Time (min)	Light Source	Yields (%) 3aa/3ab
1	10	2a	H ₂ O	30	ambient light	55
2	10	2a	H ₂ O	30	white light ^b	49
3	10	2a	H ₂ O	30	UV light ^c	76
4	10	2a	H ₂ O/EtOH ^d	30	UV light ^c	98
5	10	2a	H ₂ O	30	dark	52
6	-	2a	H ₂ O	30	UV light ^c	Trace
7	10	2b	H ₂ O	30	ambient light	ND
8	10	2b	H ₂ O	30	UV light ^c	Trace
9	10	2b	H ₂ O/EtOH ^d	30	UV light ^c	25
10	10	2b	H ₂ O/EtOH ^d	150	UV light ^c	80
11	10	2b	H ₂ O/EtOH ^d	30	dark	ND
12	-	2b	H ₂ O/EtOH ^d	30	UV light ^c	ND
13	5	2b	H ₂ O/EtOH ^d	30	UV light ^c	15

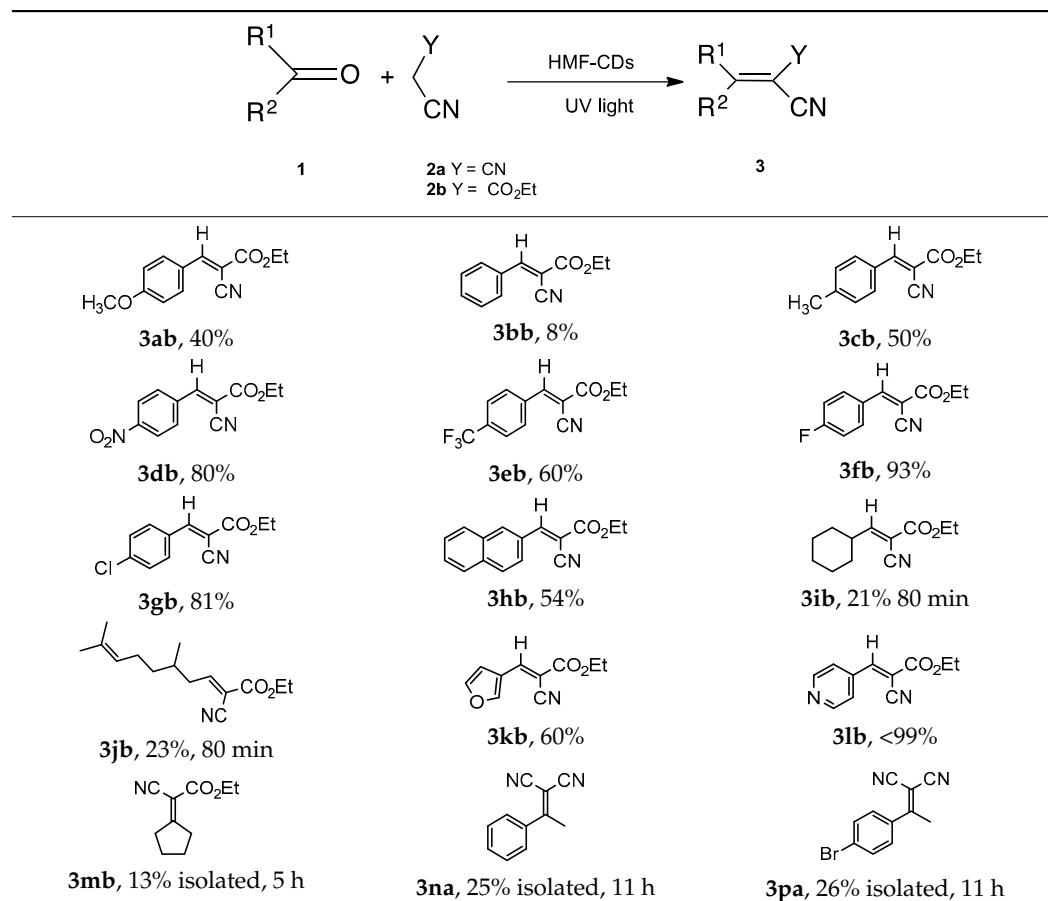
^a Reaction conditions: aldehyde **1a** (0.5 mmol), **2a/2b** (0.5 mmol), solvent (2 mL), room temperature. ^b Light irradiation (18 W, wavelength in the range 390–750 nm). ^c UV light (9W, 365 nm) ^d H₂O/EtOH (1:1). For the photochemical reaction setup, see Figure S2.

With malononitrile **2a**, which is one of the most reactive nucleophiles in the Knoevenagel condensation, the reaction proceeds under ambient or white light to give the products in 55 or 49% yields, respectively, after 30 min (Table 1, entries 1 and 2). However, in the same reaction conditions, the yield is greatly increased by UV light (9 W, 365 nm) irradiation, as shown in Table 1, entry 3, where the obtained yield was 76% using H₂O as solvent. In the presence of ethanol in a 1:1 mixture with water, an increase in yield up to 98% is observed (Table 1, entry 4). The presence of ethanol as co-solvent shifts the formation of the product further to the right, favoring the reaction. As shown in Table 1, entry 5, using malononitrile **2a** under dark conditions results in the product yield **3aa** of 52%. This is due to the intrinsic reactivity of the **2a** substrate for the Knoevenagel condensation, as reported in the literature [43]. However, in the absence of the catalyst under UV light irradiation, only a trace of **3aa** was formed which shows that the intervention of the photocatalyst integrates with the activity of the substrate (Table 1, entry 6). In the presence of the less reactive nucleophiles (**2b**) (Table 1, entries 7–13), the Knoevenagel condensation does not proceed in the absence of HMF-CDs as catalysts (Table 1, entry 12). On the other hand, when HMF-CDs were used as catalysts, the reaction proceeds under light irradiation, confirming that the HMF-CDs and irradiation are necessary for the reaction. Moreover, with the less reactive substrate **2b**, the presence of ethanol is crucial for the formation of the product. The yield of product **3ab** (80%, Table 1, entry 10) was improved when the reaction was performed in a mixed solvent of H₂O/EtOH 1:1 in 150 min under 9 W, 365 nm light irradiation. Finally, smaller amounts of catalyst loading were not beneficial for the

reaction, and neither were larger amounts due to the low solubility of HMF-CDs in the solvent mixture employed (Table 1, entry 13).

After determining the optimal reaction conditions, we investigated the range of substrates by utilizing a variety of carbonylic compounds. These substrates encompassed aliphatic and aromatic aldehydes with both electron-releasing and electron-withdrawing groups, as well as heteroaromatic aldehydes and ketones (Table 2).

Table 2. Scope of the Knoevenagel condensation reaction by photo-activated HMF-CDs as catalysts ^a.



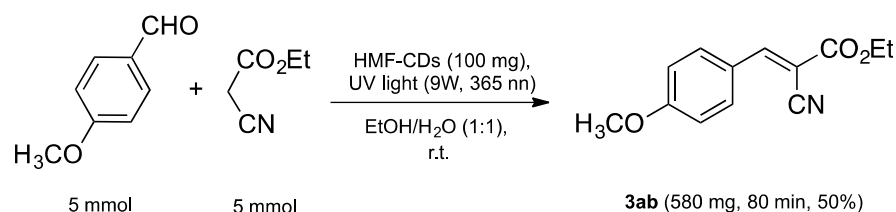
^a Reaction conditions: carbonylic compound (0.5 mmol), **2a** or **2b** (0.5 mmol), solvent H₂O/EtOH (1:1), 2 mL, r. t., UV light (9 W, 365 nm), 40 min (where unspecified). All spectroscopic data are provided in Experimental Section 3.4; Spectra data in the Supporting Information.

Intriguingly, regardless of whether aromatic or aliphatic aldehydes were used as substrates with varying functionalities, the conversions were consistently better than those observed with benzaldehyde (Table 2, **3bb**). It was revealed that the position of the substituent moiety on the phenyl ring significantly influences the reactivity. It is evident that for para-substituted benzaldehydes, the reaction proceeds with good or excellent yields at room temperature within 40 min. Aldehyde substrates with electron-withdrawing groups, such as –NO₂, –CF₃, –F, and –Cl, gave higher quantities of product (**3db**, **3eb**, **3fb**, **3gb**) compared to those with electron-donating groups like –OCH₃ and –CH₃ (**3ab**, **3cb**). Heteroaromatic aldehydes gave good to excellent yields of **3kb** and **3lb**. As reported in Table 2, the protocol is also effective for aliphatic aldehydes **3ib** and **3jb**, and ketones **3mb**, **3na**, and **3pa**, although the reactivity is lower compared to aldehydes, resulting in lower yields and longer reaction times.

An important feature of this synthetic procedure using HMF-CDs as catalysts is their ability to be recovered and recycled in subsequent runs. The reuse of HMF-CDs in the Knoevenagel reaction has been investigated, demonstrating the recycling protocol by successfully reusing the catalytic system in four consecutive runs. The reaction was carried

out under reaction conditions described in Table 2, and product **3ab** was isolated as the only product up to four times. The reaction proceeds with a slight decrease in yield, which drops from 40% to 35% in the fourth reuse cycle, confirming the usefulness of this protocol (Experimental Section 3.5, and Figure S3).

Furthermore, to demonstrate the scalability of this HMF-CD photocatalyzing Knoevenagel condensation, we carried out the model reaction on a 5 mmol scale to provide the expected product **3ab** in 50% yield in 80 min (Scheme 2). This shows that our methodology can potentially be scaled up to gram-scale synthesis (Experimental Section 3.6).



Scheme 2. Scale-up synthesis of **3ab**.

To elucidate the intermediates and steps of the reaction mechanism, several control experiments employing various quenching and trapping reagents were conducted using the less reactive nucleophile **2b** (Table 3).

Table 3. Control experiments for Knoevenagel condensation.

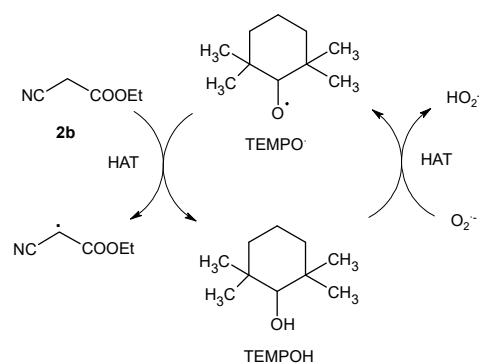
Entry	Conditions ^a	Yield (%) 3ab
1	Standard	40
2	Solvent free	48 ^b
3	H ₂ O	ND
4	Dark	Trace
5	No catalyst	3
6	N ₂	19
7	<i>p</i> -benzoquinone	25
8	TEMPO	71
9	AgNO ₃	Trace
10	HCO ₂ H	Trace

^a Standard conditions: **1a** and **2b** (0.5 mmol), 10 mg HMF-CDs H₂O/EtOH (1:1) 2 mL, 40 min, r.t., UV LED 365 nm 9 W. ^b The procedure was reported in reference [14], was carried out without a light source, and required a long reaction time (12 h). N₂: Without air oxygen; (*p*-benzoquinone 1 mmol, 2 eq): Superoxide radical anion scavenger; TEMPO (2,2,6,6-tetramethylpiperidin-1-yl)oxidanyl: Radical scavenger or hydrogen atom transfer (HAT) catalyst; AgNO₃ (0.5 mmol, 1 eq): e⁻ scavenger; HCO₂H (1.5 mmol, 3 eq): h⁺ scavenger.

Even if the comparison is between homogeneous and heterogeneous catalysis, comparing the catalytic activity of the used material can be interesting. As previously reported, the catalyst can function even without light through longer reaction times [14]. The results are reported in Table 3 (entry 1 vs. entry 2). Compared to standard conditions (Table 3, entry 1), reactions conducted using only water as the solvent or in the absence of light failed to yield the desired product **3ab** (Table 3, entries 2 and 3). This outcome underscores the significance of both light exposure and the presence of the co-solvent ethanol (a stronger base than water) for successful reaction outcomes [43]. In the presence of light but without any photocatalyst, the reactions failed to produce **3ab** in a significant yield (Table 3, entry 4). This outcome highlights the essential role of a photocatalyst for the reaction to proceed successfully. To investigate the role of oxygen in the reaction mechanism, the experiment

was performed under inert conditions (Table 3, entry 5), leading to a reduced product yield of 19%. However, in the presence of N_2 , meaning in the absence of the oxygenated reactive species that dominate the photocatalytic process, the reaction proceeds with a lower yield under the same conditions (Table 3, entry 5 vs. entry 1). This result suggests that atmospheric oxygen plays a key role in the photocatalytic process. The addition of a superoxide radical anion scavenger, *p*-benzoquinone, to the reaction mixture led to a decrease in yield, with only 25% of **3ab** generated (Table 3, entry 6). This result is consistent with the time increase of the reduced form of *p*-benzoquinone, 1,4-hydroquinone, reported in our previous investigation [39]. Experiments employing superoxide radical anion scavengers or radical scavengers and a hydrogen atom transfer (HAT) catalyst, such as TEMPO (2,2,6,6-tetramethylpiperidin-1-yl) oxidanyl, $AgNO_3$ (e^- scavenger;), and HCO_2H (h^+ scavenger), are reported in Table 3 (entries 8–10). The latter two, $AgNO_3$ and HCO_2H , prevent the reaction from proceeding, as indicated by the presence of only trace amounts of the product.

Conversely, when TEMPO was employed in the condensation (Table 3, entry 8), an unexpected increase of the product yield **3ab** was observed, suggesting the role of this compound in the mechanism (Scheme 3).



Scheme 3. Reaction between TEMPO and **2b** assisted by superoxide radical anion: the role in the mechanism.

TEMPO is widely used as a radical scavenger or oxidation catalyst. As reported in the literature, TEMPO can also catalyze hydrogen atom transfer (HAT) reactions [44,45]. Scheme 3 illustrates the role of TEMPO in relation to the C2-H of ethyl cyanoacetate (**2b**). Initially, TEMPO reacts with the C2-H of ethyl cyanoacetate to form TEMPO-H. Subsequently, TEMPO-H is converted back to TEMPO by the superoxide anion, as depicted in Scheme 3. The results of control experiments in the presence of different amounts of TEMPO are reported in Table 4.

Table 4. Control experiments: the role of TEMPO in the mechanism.

Entry	Conditions	Yield 3ab (%)
1	No catalyst	ND
2	Only CDs	Trace
3	Only UV LED	Trace
4	UV LED + TEMPO (20% mmol)	ND
5	Standard ^a	40
6	UV LED + CDs + TEMPO (20% mmol)	45
7	UV LED + CDs + TEMPO (2 eq)	71

^a Standard conditions: **1a** and **2b** (0.5 mmol), 10 mg HMF-CDs, $H_2O/EtOH$ 1:1 (2 mL), 40 min, r.t., UV LED 365 nm (9 W).

When the reaction of **1a** and **2b** was carried out in the absence of a catalyst, no product was obtained (Table 4, entry 1). The reactions between **1a** and **2b** in the presence of CDs alone or a source of light failed to give **3ab** (Table 4, entries 2 and 3). Additionally, the

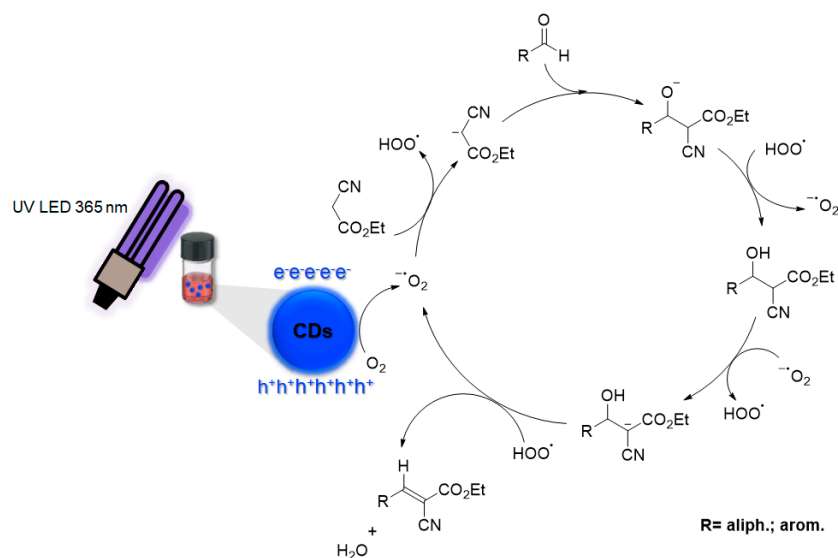
presence of TEMPO with UV light did not yield any product, indicating that CDs are essential in the photocatalytic process (Table 4, entry 4). On the other hand, compared to standard conditions, the presence of TEMPO in catalytic quantities slightly modifies the yield, with a slight increase in the quantity of the product (entry 5 vs. entry 6). Instead, as shown in Table 4, entry 7, using 2 equiv. of TEMPO, the reaction mechanism for the dehydrogenation activity of **2b**, illustrated in Scheme 3, seems to prevail over TEMPO's autoxidation capacity, thereby increasing the presence of the reactive intermediate formed from compound **2b** [44].

Accordingly, a decrease in the reaction time was also observed when the reaction mixture containing TEMPO in a 1:2 ratio respect to **2b** was analyzed by electrospray ionization mass spectrometry [39]. Then, to confirm the well-established ability of HMF-CDs to absorb UV radiation and their role in generating reactive oxygen species (ROS) through the formation of electron-hole ($e^- h^+$) pairs, as shown in Table 3, entries 9 and 10, $AgNO_3$ and formic acid were respectively introduced into the reaction mixture as e^- and h^+ scavengers. The observed partial formation of the product serves as evidence for the potential involvement of reactive oxygen species (ROS) in the reaction [20]. HMF-CDs can function as electron donors toward oxygen, leading to the formation of the superoxide radical ($O_2^{\cdot-}$), or as electron acceptors toward water, resulting in the production of the hydroxyl radical ($\cdot OH$).

As a result, the $O_2^{\cdot-}$ radical anion, in collaboration with HMF-CD catalysts, could be engaged in deprotonating the more acidic substrate, malononitrile **2a**. The superoxide ion $O_2^{\cdot-}$ is known to react with a range of organic and inorganic compounds, acting as proton donors to produce HO_2^{\cdot} [46]. Moreover, when amine-functionalized CDs are employed in the reaction, a classic base-catalyzed mechanism is invoked [30]. It is thus reasonable that the reaction between an aldehyde and malononitrile, one of the most reactive methylene-activated compounds, could proceed via the classic base-catalyzed Knoevenagel condensation through the formation of an aldol intermediate [47]. Interestingly, in the presence of **2a**, the condensation yield (**3aa**) was slightly lower when the reaction mixture was not exposed to a light source, suggesting that the intervention of the superoxide radical anion in the basic catalysis is minimally necessary to the formation of the final product when malononitrile **2a** is employed (Table 1, entry 4) [48]. It is expected that replacing malononitrile with ethyl cyanoacetate can significantly reduce the reactivity of the reaction mixture. This is attributed to the lower acidity of ethyl cyanoacetate compared to malononitrile, which could hinder the formation of the aldolic intermediate, thereby impacting the progression of the reaction [48,49].

Conversely, a significant rise in the yield of the condensation reaction was noted when ethyl cyanoacetate **2b** and the HMF-CD catalysts were exposed to UV irradiation at a wavelength of 365 nm compared to the reaction conducted in the absence of light (Table 1, entry 9 vs. 11). Therefore, by employing ethyl cyanoacetate **2b**, the participation of the superoxide radical anion in the catalysis promotes the reaction between the aldehyde substrates and **2b** in a radical-driven reaction (Scheme 4). In this scenario, the less efficient base-catalyzed mechanism, due to the lower acidity of **2b**, can benefit from the intervention of $O_2^{\cdot-}$ radical anion that is generated when a UV light source activates the HMF-CD catalysts. These results are in good agreement with the findings of our previous study [39], thus reconciling the synthetic data with the mechanistic mass spectrometric evidence on the key role played by the $O_2^{\cdot-}$ radical anion in the formation of the product.

The photocatalytic mechanism was further validated through a light on-off experiment. The experiment was conducted by alternating 30-min intervals of stirring in the dark with 20-min periods of stirring under UV (365 nm) irradiation on a $MeOD-d_4/D_2O$ mixture containing substrate **1a**, **2b** and HMF-CDs. As shown in Figure 2, exposure of the reaction mixture containing the HMF-CD photocatalyst to UV light results in an increase in yield during the light-on steps.



Scheme 4. Mechanism hypothesized for the reaction photocatalyzed by HMF-CDs and mediated by $O_2^{\bullet -}$.

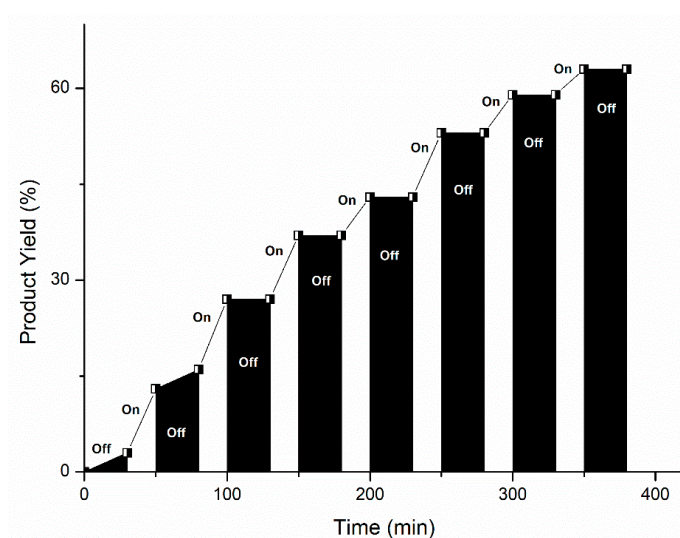


Figure 2. Light on–off experiment for the standard reaction. The procedure is described in Experimental Section 3.8.

At the beginning of the light on–off experiment, the reaction proceeds with a low yield for up to 80 min. This is due to the catalyst’s activity, which slightly increases the product yield even in the absence of light. However, the yield increases significantly in the presence of light (Figure 2). After this time, when the UV light is turned off, the reaction yield remains constant. This indicates that, in the absence of light, the photocatalytic species involved in the reaction are not formed. This conclusion is supported by the yield reported under dark conditions in Table 3, entry 4. Therefore, the experimental findings shown in Figure 2 align with expectations, indicating that light is essential for achieving higher yields and shorter reaction times.

3. Experimental

3.1. General Information

All reagents and all solvents used in this study were analytical-grade reagents purchased from Sigma-Aldrich and used as received without further purification. Ultrapure water ($18.2 \text{ M}\Omega \text{ cm}^{-1}$) from a Milli-Q ultrapure system was used in this study.

NMR spectra were recorded at ambient temperature on Bruker spectrometers operating at 400 MHz or on a Spinsolve 60 spectrometer operating at 60 MHz using the solvent as an internal standard. The chemical shifts (δ) are given in ppm relative to TMS. Melting point measurements were determined using Melting Point Apparatus SMP 2 Stuart Scientific. Accurate mass measurements were performed by using a 2D-UHPLC Agilent 1290 Infinity II coupled with a 6546 LC/Q-TOF system from Agilent Technologies (Santa Clara, CA, USA). Mass spectra were processed by using Agilent Mass Hunter Qualitative Analysis version 10.0. UV-Vis absorption spectra were performed with Agilent 8453 Spectrophotometer Agilent ChemStation for UV-Visible Spectroscopy.

3.2. Photochemical Setup

The photoreactor utilized for the Knoevenagel condensation includes a 365 nm LED lamp (9 W) (see Figure S2). The reaction vial was positioned 2 cm away from the LED lamp and housed within an aluminum enclosure. The sample was irradiated with a 365 nm LED light source, while cooling was facilitated by a fan to maintain the system at room temperature.

3.3. General Procedures for the Synthesis of 5HMF-Derived CDs

The electrochemical synthesis of 5HMF-derived CDs (HMF-CDs) was performed in a glass vial by adding 5 mL of NH_4OH (30%) aqueous solution containing 200.0 mg (1.6 mmol) of 5HMF. A static potential (8 V) was applied to the mixture through two platinum spiral wires (1 cm^2 apparent area) for 2.5 h at room temperature (25 °C). Afterwards, the mixture was centrifuged (6000 rpm, 10 min) and the supernatant was dialyzed using a dialysis membrane (MWCO 0.1–0.5 kD) against ultrapure water for 72 h, changing it every 24 h. HMF-CDs were isolated from evaporating water under vacuum. The HMF-CD samples underwent characterization using various techniques. All data related to this characterization were previously reported [14]. For the electrochemical synthesis of HMF-CDs, process efficiency indicators (PEM) were evaluated [50]. As also reported for the synthesis of carbon dots from biomass [51], our attention was directed to the key parameters: mass intensity (MI), mass productivity (MP), and environmental impact factor (E-factor). The results are reported in Table S1. The E-factor parameter yielded a value of 6 (with the optimum value being 1). Notably, literature data often indicate that E-factors for industrial processes related to fine chemical production typically range from 5 to 50.

3.4. General Procedure for the Synthesis of **3ab–pa**

In a vial, HMF-CDs (10 mg) were diluted in a 2 mL solution of $\text{H}_2\text{O}/\text{EtOH}$ (1:1), followed by sonication for 15 min. Subsequently, compounds **1a–p** (0.5 mmol, 1 eq) and **2b** (0.5 mmol, 53 μL , 1 eq) were introduced into the mixture. The vial was positioned in the photoreactor and stirred for 40 min–11 h under UV (365 nm) irradiation. The reaction was quenched by adding 3 mL of H_2O and extracted with ethyl acetate (3 \times 4 mL). The organic layer was separated and dried with Na_2SO_4 , filtered, and concentrated at reduced pressure.

Products 3ab–3hb, 3kb–3lb: The vial was positioned in the photoreactor and stirred for 40 min under UV (365 nm) irradiation. The reaction was quenched by adding 3 mL of H_2O and extracted with ethyl acetate (3 \times 4 mL). The organic layer was separated and dried with Na_2SO_4 , filtered, and concentrated at reduced pressure.

Products 3ib–3jb: The vial was positioned in the photoreactor and stirred for 80 min under UV (365 nm) irradiation. The reaction was quenched by adding 3 mL of H_2O and extracted with ethyl acetate (3 \times 4 mL). The organic layer was separated and dried with Na_2SO_4 , filtered, and concentrated at reduced pressure.

Product 3mb: The vial was positioned in the photoreactor and stirred for 5 h under UV (365 nm) irradiation. The reaction was quenched by adding 3 mL of H_2O and extracted with ethyl acetate (3 \times 4 mL). The organic layer was separated and dried with Na_2SO_4 , filtered, and concentrated at reduced pressure. The crude products were purified by column chromatography on silica gel using petroleum ether/ethyl acetate (5:1) as eluent.

Products **3na–3pa**: The vial was positioned in the photoreactor and stirred for 11 h under UV (365 nm) irradiation. The reaction was quenched by adding 3 mL of H₂O and extracted with ethyl acetate (3 × 4 mL). The organic layer was separated and dried with Na₂SO₄, filtered, and concentrated at reduced pressure. The collected solid was recrystallized from ethanol or hot ethanol/water (3:2).

The obtained products gave spectral data in accordance with those reported in the literature, except for compound **3jb**, which has been characterized by ¹H and ¹³C NMR and monoisotopic mass. The spectral data are provided in Supporting Information.

3.4.1. Ethyl(*E*)-2-cyano-3-(4-methoxyphenyl)acrylate (**3ab**)

White solid; mp: 79–81 °C; ¹H NMR (400.13 MHz, CDCl₃) δ 8.15 (s, 1H), 7.98 (d, *J* = 8.9 Hz, 2H), 6.98 (d, *J* = 8.9 Hz, 2H), 4.35 (q, *J* = 7.1 Hz, 2H), 3.88 (s, 3H), 1.37 (t, *J* = 7.1 Hz, 3H). ¹³C NMR (100.6 MHz, CDCl₃) δ 163.87, 163.20, 154.47, 133.73, 124.44, 116.32, 114.85, 99.42, 62.51, 55.71, 14.29. The characterization data matched the literature [52].

3.4.2. Ethyl(*E*)-2-cyano-3-phenylacrylate (**3bb**)

White solid; mp: 54–55 °C; ¹H NMR (400.13 MHz, CDCl₃) δ 8.25 (s, 1H), 7.99 (d, *J* = 7.5 Hz, 2H), 7.59–7.45 (m, 3H), 4.39 (q, *J* = 7.1 Hz, 2H), 1.40 (t, *J* = 7.1 Hz, 3H). ¹³C NMR (100.6 MHz, CDCl₃) δ 162.52, 155.10, 133.34, 131.49, 131.09, 129.30, 115.51, 103.02, 62.77, 14.18. The characterization data matched the literature [53].

3.4.3. Ethyl(*E*)-2-cyano-3-(*p*-tolyl)acrylate (**3cb**)

White solid; mp: 90–92 °C; ¹H NMR (400.13 MHz, CDCl₃) δ 8.21 (s, 1H), 7.90 (d, *J* = 8.2 Hz, 2H), 7.30 (d, *J* = 8.1 Hz, 2H), 4.38 (q, *J* = 7.1 Hz, 2H), 2.43 (s, 3H), 1.39 (t, *J* = 7.1 Hz, 3H). ¹³C NMR (100.6 MHz, CDCl₃) δ 162.81, 155.04, 144.68, 131.28, 130.06, 128.90, 115.81, 101.59, 62.62, 21.89, 14.20. The characterization data matched the literature [54].

3.4.4. Ethyl(*E*)-2-cyano-3-(4-nitrophenyl)acrylate (**3db**)

Yellow solid; mp: 167–168 °C; ¹H NMR (400.13 MHz, CDCl₃) δ 8.35 (d, *J* = 8.8 Hz, 2H), 8.30 (s, 1H), 8.13 (d, *J* = 8.8 Hz, 2H), 4.42 (q, *J* = 7.1 Hz, 2H), 1.42 (t, *J* = 7.1 Hz, 3H). ¹³C NMR (100.6 MHz, CDCl₃) δ 161.43, 151.76, 149.73, 136.92, 131.53, 124.34, 114.55, 107.39, 63.3, 14.12. The characterization data matched the literature [55].

3.4.5. Ethyl(*E*)-2-cyano-3-(4-(trifluoromethyl)phenyl)acrylate (**3eb**)

White solid; mp 110–112 °C; ¹H NMR (400.13 MHz, CDCl₃) δ 8.28 (s, 1H), 8.08 (d, *J* = 8.2 Hz, 2H), 7.76 (d, *J* = 8.4 Hz, 2H), 4.41 (q, *J* = 7.1 Hz, 2H), 1.41 (t, *J* = 7.1 Hz, 3H). ¹³C NMR (100.6 MHz, CDCl₃) δ 161.86, 153.05, 134.61, 134.08, 131.06, 126.28 (q, *J* = 3.8 Hz), 124.78, 122.07, 114.89, 106.00, 63.21, 14.19. The characterization data matched the literature [56].

3.4.6. Ethyl(*E*)-2-cyano-3-(4-fluorophenyl)acrylate (**3fb**)

Yellow solid; mp 95–97 °C; ¹H NMR (400.13 MHz, CDCl₃) δ 8.21 (s, 1H), 8.07–7.98 (m, 2H), 7.19 (t, *J* = 8.6 Hz, 2H), 4.38 (q, *J* = 7.1 Hz, 2H), 1.40 (t, *J* = 7.1 Hz, 3H). ¹³C NMR (100.6 MHz, CDCl₃) δ 166.70, 164.14, 162.42, 153.52, 133.61 (d, *J* = 9.3 Hz), 127.86 (d, *J* = 3.3 Hz), 116.84, 116.62, 115.46, 102.59 (d, *J* = 2.4 Hz), 62.82, 14.16. The characterization data matched the literature [57].

3.4.7. Ethyl(*E*)-3-(4-chlorophenyl)-2-cyanoacrylate (**3gb**)

White solid; mp 92–93 °C; ¹H NMR (400.13 MHz, CDCl₃) δ 8.19 (s, 1H), 7.93 (d, *J* = 8.6 Hz, 2H), 7.48 (d, *J* = 8.6 Hz, 2H), 4.38 (q, *J* = 7.1 Hz, 2H), 1.40 (t, *J* = 7.1 Hz, 3H). ¹³C NMR (100.6 MHz, CDCl₃) δ 162.26, 153.43, 139.62, 132.22, 129.89, 129.70, 115.29, 103.50, 62.90, 14.16. The characterization data matched the literature [58].

3.4.8. Ethyl(*E*)-2-cyano-3-(naphthalen-2-yl)acrylate (**3hb**)

White solid; mp 112–114 °C; ¹H NMR (400.13 MHz, CDCl₃) δ 8.40 (s, 1H), 8.38 (s, 1H), 8.19 (dd, *J* = 8.7, 1.6 Hz, 1H), 7.90 (dd, *J* = 18.5, 8.2 Hz, 2H), 7.66–7.51 (m, 2H), 4.41 (q, *J* = 7.1 Hz, 2H), 1.42 (t, *J* = 7.1 Hz, 3H). ¹³C NMR (100.6 MHz, CDCl₃) δ 162.71, 155.02, 135.43, 134.21, 132.83, 129.44, 129.20, 129.13, 129.08, 127.90, 127.25, 125.30, 115.79, 102.67, 62.76, 14.22. The characterization data matched the literature [59].

3.4.9. Ethyl(*E*)-2-cyano-3-(furan-3-yl)acrylate (**3kb**)

Light brown solid; mp 93–94 °C; ¹H NMR (400.13 MHz, CDCl₃) δ 8.00 (s, 1H), 7.73 (s, 1H), 7.38 (d, *J* = 3.5 Hz, 1H), 6.71–6.60 (m, 1H), 4.34 (q, *J* = 7.1 Hz, 2H), 1.37 (t, *J* = 7.1 Hz, 3H). ¹³C NMR (100.6 MHz, CDCl₃) δ 162.62, 148.77, 148.27, 139.51, 121.73, 115.37, 113.86, 98.68, 62.60, 14.19. The characterization data matched the literature [60].

3.4.10. Ethyl(*E*)-2-cyano-3-cyclohexylacrylate (**3ib**)

Yellow oil; ¹H NMR (400.13 MHz, CDCl₃) δ 7.45 (d, *J* = 10.5 Hz, 1H), 4.28 (q, *J* = 7.1 Hz, 2H), 2.75–2.58 (m, 1H), 1.77–1.68 (m, 4H), 1.36–1.17 (m, 9H). ¹³C NMR (100.6 MHz, CDCl₃) δ 167.87, 161.58, 113.77, 107.57, 62.39, 41.10, 31.08, 25.35, 24.82, 14.08. The characterization data matched the literature [60].

3.4.11. Ethyl(*E*)-2-cyano-5,9-dimethyldeca-2,8-dienoate (**3jb**)

Colorless oil; ¹H NMR (400.13 MHz, CDCl₃) δ 7.66 (t, *J* = 8.0 Hz, 1H), 5.14–5.02 (m, 1H), 4.31 (q, *J* = 7.1 Hz, 2H), 2.56 (ddd, *J* = 13.5, 7.6, 5.8 Hz, 1H), 2.48–2.35 (m, 1H), 1.99 (dt, *J* = 23.1, 7.1 Hz, 2H), 1.82–1.72 (m, 1H), 1.68 (s, 3H), 1.60 (s, 3H), 1.35 (t, *J* = 7.1 Hz, 3H), 1.32–1.24 (m, 2H), 0.96 (d, *J* = 6.7 Hz, 3H). ¹³C NMR (100.6 MHz, CDCl₃) δ 163.11, 161.40, 132.07, 123.97, 113.95, 110.61, 62.54, 39.23, 36.83, 32.54, 25.83, 25.53, 19.67, 17.81, 14.21. Measured monoisotopic mass [C₁₅H₂₃NO₂+H]⁺: *m/z* 250.1806 (theoretical monoisotopic mass [C₁₅H₂₃NO₂+H]⁺: *m/z* 250.1729; Δ: 1.7 ppm).

3.4.12. Ethyl(*E*)-2-cyano-3-(pyridin-4-yl)acrylate (**3lb**)

Pink solid; mp 103–105 °C; ¹H NMR (400.13 MHz, CDCl₃) δ 8.75 (dd, *J* = 4.6, 1.5 Hz, 2H), 8.12 (s, 1H), 7.68 (dd, *J* = 4.7, 1.4 Hz, 2H), 4.35 (q, *J* = 7.1 Hz, 2H), 1.34 (t, *J* = 7.1 Hz, 3H). ¹³C NMR (100.6 MHz, CDCl₃) δ 161.30, 152.14, 151.15, 138.06, 123.28, 114.27, 108.33, 63.36, 14.11. The characterization data matched the literature [60].

3.4.13. Ethyl 2-cyano-2-cyclopentylideneacetate (**3mb**)

Yellow oil; ¹H NMR (400.13 MHz, CDCl₃) δ 4.27 (q, *J* = 7.1 Hz, 2H), 2.99 (t, *J* = 6.9 Hz, 2H), 2.80 (t, *J* = 6.8 Hz, 2H), 1.98–1.70 (m, 4H), 1.34 (t, *J* = 7.1 Hz, 3H). ¹³C NMR (100.6 MHz, CDCl₃) δ 187.62, 162.10, 115.76, 100.97, 61.69, 37.94, 35.61, 26.71, 25.25, 14.31. The characterization data matched the literature [61].

3.4.14. 2-(1-phenylethylidene)malononitrile (**3na**)

White solid; mp 96–98 °C; ¹H NMR (400.13 MHz, CDCl₃) δ 7.59–7.48 (m, 5H), 2.64 (s, 3H). ¹³C NMR (100.6 MHz, CDCl₃) δ 175.55, 135.92, 132.32, 129.16, 127.37, 112.82, 112.75, 84.74, 24.3. The characterization data matched the literature [62].

3.4.15. 2-(1-(4-bromophenyl)ethylidene)malononitrile (**3pa**)

White solid; mp 97–99 °C; ¹H NMR (400.13 MHz, CDCl₃) δ 7.65 (d, *J* = 8.6 Hz, 2H), 7.43 (d, *J* = 8.6 Hz, 2H), 2.62 (s, 3H). ¹³C NMR (100.6 MHz, CDCl₃) δ 174.06, 134.74, 132.66, 128.99, 127.30, 112.68, 112.59, 85.36, 24.27. The characterization data matched the literature [63].

3.5. Reusability of the Catalyst

The described procedure can also provide the reusability of HMF-CDs for at least four consecutive runs without significant impact in terms of product yields. Therefore, to test the possibility to recycle, the HMF-CDs were used as catalysts for subsequent catalytic runs

under standard conditions with compounds **1a** and **2b**. Experiments for reusability of the catalyst were performed following the standard conditions: **1a** and **2b** (0.5 mmol), 10 mg HMF-CDs H₂O/EtOH (1:1) 2 mL, 40 min, r.t., UV LED 365 nm 9W. After each cycle, the organic product **3ab** was removed from the reaction (as reported above), and the HMF-CD was washed once with EtOH and dried under vacuum. The results obtained for four runs are reported in Figure S3 of the Supporting Information.

3.6. Scale Up Procedure

In a glass tube, HMF-CDs (100 mg) were diluted in a 20 mL solution of H₂O/EtOH (1:1), followed by sonication for 15 min. Subsequently, compounds **1a** (5 mmol, 624 μ L, 1 eq) and **2b** (5 mmol, 530 μ L, 1 eq) were introduced into the mixture. The mixture was positioned in the photoreactor and stirred for 80 min under UV (365 nm) irradiation. The reaction was quenched by adding 10 mL of H₂O and extracted with ethyl acetate (3 \times 30 mL). The organic layer was separated and dried with Na₂SO₄, filtered, and concentrated at reduced pressure.

3.7. Mechanistic Investigations

Experiments for mechanistic investigations were performed following the standard procedure (Table 3, entry 1): in a glass tube, HMF-CDs (10 mg) were diluted in a 2 mL solution of H₂O/EtOH (1:1), followed by sonication for 15 min. Then, compounds **1a** (0.5 mmol, 62 μ L, 1 eq) and **2b** (0.5 mmol, 53 μ L, 1 eq) were introduced into the mixture. The vial was positioned in the photoreactor and stirred for 40 min under UV (365 nm) irradiation. The reaction was quenched by adding 3 mL of H₂O and extracted with ethyl acetate (3 \times 4 mL). The organic layer was separated and dried with Na₂SO₄, filtered, and concentrated at reduced pressure. The reaction was also carried out without solvent (Table 3, entry 2); the reaction conditions were reported in ref. [14].

When the reaction was performed using water as solvent, 10 mg of HMF-CDs were diluted in 2 mL of water and sonicated for 15 min (Table 3, entry 3).

In dark conditions, the vial with the reaction mixture was covered with foil and then stirred for the specified time (Table 3, entry 4).

The reaction was also carried out in the same conditions of entry 1 without a catalyst (Table 3, entry 5) and under inert conditions (Table 3, entry 6); the vial was flamed under N₂ flux before the reactants were added.

Experiments employing different radical scavengers were performed by alternatively adding to the reaction mixtures *p*-benzoquinone, (2,2,6,6-tetramethylpiperidin-1-yl)oxidanyl (TEMPO), AgNO₃ (1 eq), and HCOOH (3 eq) (Table 3, entries 7–10).

3.8. Light On–Off Experiment

Two mg of HMF-CDs were diluted in a MeOD-*d*₄ (0.75 mL) and D₂O (0.1 mL) solution and sonicated for 15 min. Then, **1a** (0.1 mmol, 12 μ L, 1 eq) and **2b** (0.1 mmol, 11 μ L, 1 eq) were introduced into the solution, and the mixture was transferred into an NMR glass tube. The experiment was conducted by alternating 30 min intervals of stirring in the dark, with 20 min periods of stirring under UV (365 nm) irradiation. After each time interval, a ¹H NMR spectrum was recorded. The product yield was determined by using the MeOH residual peak as internal reference.

4. Conclusions

Advances in photocatalysis applications were studied to provide new insights for applications employing CD-based photoinduced chemical reactions. The Knoevenagel condensation photocatalyzed by HMF-CDs was studied. The chemistry is driven by the ability of HMF-CDs to act as both bases and photo-active species, and the intervention in the process of the superoxide radical anion was analyzed. The reaction was studied with ethyl cyanoacetate and malononitrile and proved suitable with aromatic aldehydes, having both electron donation and electron withdrawal substituents, aliphatic and heteroaromatic

aldehydes, and ketones. The reaction was studied with ethyl cyanoacetate and malononitrile. The sustainable nature of the HMF-CDs was evidenced by their ability to be recycled up to four times without significant loss of activity. This procedure was used for scaling up reactions, thereby underscoring its potential for industrial applications.

Supplementary Materials: The following supporting information can be downloaded at <https://www.mdpi.com/article/10.3390/photochem4030022/s1>, Figure S1. UV-visible absorption spectrum of HMF-CDs; Figure S2. Photochemical setup; Figure S3. Reusability of HMF-CDs catalyst; Table S1. Process Efficient Metrics calculations; ^1H and ^{13}C NMR Spectra.

Author Contributions: Conceptualization, I.C. and A.T.; methodology, C.M. and C.S.; investigation, C.M. and C.S.; resources, I.C., A.T. and F.S.; writing—original draft preparation, I.C., A.T., C.M. and C.S.; writing—review and editing, I.C., A.T. and C.S.; visualization, I.C., A.T., C.M. and C.S.; supervision, I.C., A.T. and F.P.; project administration, I.C., A.T. and F.P.; funding acquisition, I.C., A.T. and F.P. All authors have read and agreed to the published version of the manuscript.

Funding: This research was funded by “Progetti di Ateneo” grant number: RM120172A8223162.

Data Availability Statement: The datasets generated and analyzed during the present study are available from the corresponding author on request.

Acknowledgments: C.S. and C.M. thank the Italian Ministry of University and Research (MUR) for a Researcher position (DM n. 1062, 10 August 2021) and a PhD position (DM n. 1061, 10 August 2021) within the EU-funded National Operational Programme (PON) on Research and Innovation 2014–2020.

Conflicts of Interest: All authors declare no conflict of interest.

References

1. Anastas, P.T.; Kirchhoff, M.M. Origins, current status, and future challenges of green chemistry. *Acc. Chem. Res.* **2002**, *35*, 686–694. [[CrossRef](#)] [[PubMed](#)]
2. Michelin, C.; Hoffmann, N. Photosensitization and photocatalysis—Perspectives in organic synthesis. *ACS Catal.* **2018**, *8*, 12046–12055. [[CrossRef](#)]
3. Liu, J.; Li, R.; Yang, B. Carbon dots: A new type of carbon-based nanomaterial with wide applications. *ACS Cent. Sci.* **2020**, *6*, 2179–2195. [[CrossRef](#)]
4. Lim, S.Y.; Shen, W.; Gao, Z. Carbon quantum dots and their applications. *Chem. Soc. Rev.* **2015**, *44*, 362–381. [[CrossRef](#)] [[PubMed](#)]
5. Das, P.; Maity, P.P.; Ganguly, S.; Ghosh, S.; Baral, J.; Bose, M.; Choudhary, S.; Gangopadhyay, S.; Dhara, S.; Das, A.K.; et al. Biocompatible carbon dots derived from κ -carrageenan and phenyl boronic acid for dual modality sensing platform of sugar and its anti-diabetic drug release behavior. *Int. J. Biol. Macromol.* **2019**, *132*, 316–329. [[CrossRef](#)]
6. Shahraki, H.S.; Ahmad, A.; Bushra, R. Green carbon dots with multifaceted applications—Waste to wealth strategy. *Flat Chem.* **2022**, *31*, 100310. [[CrossRef](#)]
7. Kang, C.; Huang, Y.; Yang, H.; Yan, X.F.; Chen, Z.P. A review of carbon dots produced from biomass wastes. *Nanomaterials* **2020**, *10*, 2316. [[CrossRef](#)] [[PubMed](#)]
8. Kurian, M.; Paul, A. Recent trends in the use of green sources for carbon dot synthesis—A short review. *Carbon Trends* **2021**, *3*, 100032. [[CrossRef](#)]
9. Khairul Anuar, N.K.; Tan, H.L.; Lim, Y.P.; So’aib, M.S.; Bakar, N.F. A review on multifunctional carbon dots synthesized from biomass waste: Design/fabrication, characterization and applications. *Front. Energy Res.* **2021**, *9*, 626549. [[CrossRef](#)]
10. Gao, Y.; Ge, L.; Xu, H.; Davey, K.; Zheng, Y.; Qiao, S.-Z. Electrocatalytic refinery of biomass-based 5-hydroxymethylfurfural to fine chemicals. *ACS Catal.* **2023**, *13*, 11204–11231. [[CrossRef](#)]
11. Li, Z.; Yuan, Y.; Yao, Y.; Wei, X.; Yue, T.; Meng, J. Formation of 5-hydroxymethylfurfural in industrial-scale apple juice concentrate processing. *Food Control* **2019**, *102*, 56–68. [[CrossRef](#)]
12. Bressi, V.; Chiarotto, I.; Ferlazzo, A.; Celesti, C.; Michenzi, C.; Len, T.; Iannazzo, D.; Neri, G.; Espro, C. Voltammetric sensor based on waste-derived carbon nanodots for enhanced detection of nitrobenzene. *ChemElectroChem* **2023**, *10*, e202300004. [[CrossRef](#)]
13. Rosso, C.; Filippini, G.; Prato, M. Carbon dots as nano-organocatalysts for synthetic applications. *ACS Catal.* **2020**, *10*, 8090–8105. [[CrossRef](#)]
14. Michenzi, C.; Espro, C.; Bressi, V.; Celesti, C.; Vetica, F.; Salvitti, C.; Chiarotto, I. Electrochemical *bottom-up* synthesis of biomass-derived carbon dots for promoting Knoevenagel condensation. *Mol. Catal.* **2023**, *544*, 113182. [[CrossRef](#)]
15. Lang, X.; Chen, X.; Zhao, J. Heterogeneous visible light photocatalysis for selective organic transformations. *Chem. Soc. Rev.* **2014**, *43*, 473–486. [[CrossRef](#)] [[PubMed](#)]
16. Saini, D.; Garg, A.K.; Dalal, C.; Anand, S.R.; Sunkar, S.K.; Sonker, A.K.; Westman, G. Visible-light-promoted photocatalytic applications of carbon dots: A review. *ACS Appl. Nano Mater.* **2022**, *5*, 3087–3109. [[CrossRef](#)]

17. Munir, S.; Dionysiou, D.D.; Khan, S.B.; Shah, S.M.; Adhikari, B.; Shah, A. Development of photocatalysts for selective and efficient organic transformations. *J. Photochem. Photobiol. B* **2015**, *148*, 209–222. [[CrossRef](#)] [[PubMed](#)]
18. Garbarino, S.; Ravelli, D.; Protti, S.; Basso, A. Photoinduced multicomponent reactions. *Angew. Chem. Int. Ed.* **2016**, *55*, 15476–15484. [[CrossRef](#)]
19. Yu, Y.; Zeng, Q.; Tao, S.; Xia, C.; Liu, C.; Liu, P.; Yang, B. Carbon dots based photoinduced reactions: Advances and perspective. *Adv. Sci.* **2023**, *10*, 2207621. [[CrossRef](#)]
20. Wang, X.; Cao, L.; Lu, F.; Meziani, M.J.; Li, H.; Qi, G.; Zhou, B.; Harruff, B.A.; Kermarrec, F.; Sun, Y.-P. Photoinduced electron transfers with carbon dots. *Chem. Commun.* **2009**, *25*, 3774–3776. [[CrossRef](#)]
21. Crisenza, G.E.M.; Melchiorre, P. Chemistry glows green with photoredox catalysis. *Nat. Commun.* **2020**, *11*, 803. [[CrossRef](#)]
22. Wang, W.; Luo, M.; Yao, W.; Ma, M.; Pullarkat, S.A.; Xu, L.; Leung, P.-H. Catalyst-free and solvent-free cyanosilylation and Knoevenagel condensation of aldehydes. *ACS Sustain. Chem. Eng.* **2019**, *7*, 1718–1722. [[CrossRef](#)]
23. Kotnik, T.; Žerjav, G.; Pintar, A.; Žagar, E.; Kovačič, S. Highly porous poly(arylene cyano-vinylene) beads derived through the Knoevenagel condensation of the Oil-in-Oil-in-Oil double emulsion templates. *ACS Macro Lett.* **2021**, *10*, 1248–1253. [[CrossRef](#)]
24. Cao, X.; Li, Y.; Liu, B.; Gao, A.; Cao, J.; Yu, Y.; Hei, X. A fluorescent conjugated polymer photocatalyst based on the Knoevenagel polycondensation for hydrogen production. *New J. Chem.* **2019**, *43*, 7093–7098. [[CrossRef](#)]
25. Gambacorta, G.; Sharley, J.S.; Baxendale, I.R. A comprehensive review of flow chemistry techniques tailored to the flavours and fragrances industries. *Belstein J. Org. Chem.* **2021**, *17*, 1181–1312. [[CrossRef](#)]
26. Dieter, M.Z.; Freshwater, S.L.; Solis, W.A.; Nebert, D.W.; Dalton, T.P. Tryphostin AG879, a tyrosine kinase inhibitor: Prevention of transcriptional activation of the electrophile and the aromatic hydrocarbon response elements. *Biochem. Pharmacol.* **2001**, *61*, 215–225. [[CrossRef](#)]
27. Beutler, U.; Fuenfschilling, P.C.; Steinkemper, A. An improved manufacturing process for the antimalaria drug coartem. Part II. *Org. Process Res. Dev.* **2007**, *11*, 341–345. [[CrossRef](#)]
28. Tokala, R.; Bora, D.; Shankara, N. Contribution of Knoevenagel condensation products toward the development of anticancer agents: An updated review. *ChemMedChem* **2022**, *17*, e202100736. [[CrossRef](#)]
29. Magaji, B.; Singh, P.; Skelton, A.A.; Martincigh, B.S. Synthesis, photostability and antibacterial activity of a series of symmetrical α,β -unsaturated ketones as potential UV filters. *J. Photochem. Photobiol. A* **2023**, *445*, 115018. [[CrossRef](#)]
30. Dalessandro, E.V.; Collin, H.P.; Valle, M.S.; Pliego, J.R., Jr. Mechanism and free energy profile of base catalyzed Knoevenagel condensation reaction. *RSC Adv.* **2016**, *6*, 57803–57810. [[CrossRef](#)]
31. Pandolfi, F.; Feroci, M.; Chiarotto, I. Role of anion and cation in the 1-methyl-3-butyl imidazolium ionic liquids BMImX: The Knoevenagel condensation. *ChemistrySelect* **2018**, *3*, 4745–4749. [[CrossRef](#)]
32. Salvitti, C.; Pepi, F.; Managò, M.; Bortolami, M.; Michenzi, C.; Chiarotto, I.; Troiani, A.; de Petris, G. Free *N*-heterocyclic carbenes from Brønsted acidic ionic liquids: Direct detection by electrospray ionization mass spectrometry. *Rapid Commun. Mass Spectrom.* **2022**, *36*, e9338. [[CrossRef](#)] [[PubMed](#)]
33. Salvitti, C.; Chiarotto, I.; Pepi, F.; Troiani, A. Charge-tagged *N*-heterocyclic carbenes (NHCs): Revealing the hidden side of NHC-catalysed reactions through electrospray ionization mass spectrometry. *ChemPlusChem* **2021**, *86*, 209–223. [[CrossRef](#)] [[PubMed](#)]
34. Troiani, A.; de Petris, G.; Pepi, F.; Garzoli, S.; Salvitti, C.; Rosi, M.; Ricci, A. Base-assisted conversion of protonated D-fructose to 5-HMF: Searching for gas-phase green models. *ChemistryOpen* **2019**, *8*, 1190–1198. [[CrossRef](#)]
35. Salvitti, C.; Bortolami, M.; Chiarotto, I.; Troiani, A.; de Petris, G. The Knoevenagel condensation catalysed by ionic liquids: A mass spectrometric insight into the reaction mechanism. *New J. Chem.* **2021**, *45*, 17787–17795. [[CrossRef](#)]
36. Appaturi, J.N.; Ratti, R.; Phoon, B.L.; Batagarawa, S.M.; Din, I.U.; Selvaraj, M.; Ramalingam, R.J. A review of the recent progress on heterogeneous catalysts for Knoevenagel condensation. *Dalton Trans.* **2021**, *50*, 4445–4469. [[CrossRef](#)]
37. Zhang, M.; Chen, M.-N.; Li, J.-M.; Liu, N.; Zhang, Z.-H. Visible-light initiated one-pot, three-component synthesis of 2-amino-4H-pyran-3,5-dicarbonitrile derivatives. *ACS Comb. Sci.* **2019**, *21*, 685–691. [[CrossRef](#)]
38. Das, A.; Justin Thomas, K.R. Rose bengal photocatalyzed Knoevenagel condensation of aldehydes and ketones in aqueous medium. *Green Chem.* **2022**, *24*, 4952–4957. [[CrossRef](#)]
39. Cosentino, F.; Michenzi, C.; Di Noi, A.; Salvitti, C.; Pepi, F.; de Petris, G.; Chiarotto, I.; Troiani, A. Photo-activated Carbon dots (CDs) as catalysts in the Knoevenagel condensation: A mechanistic study by dual-mode monitoring via ESI-MS. *ChemPlusChem* **2024**, *89*, e202400174. [[CrossRef](#)]
40. Han, Y.; Huang, H.; Zhang, H.; Liu, Y.; Han, X.; Liu, R.; Li, H.; Kang, Z. Carbon quantum dots with photoenhanced hydrogen-bond catalytic activity in aldol condensations. *ACS Catal.* **2014**, *4*, 781–787. [[CrossRef](#)]
41. Pei, X.; Xiong, D.; Wang, H.; Gao, S.; Zhang, X.; Zhang, S.; Wang, J. Reversible phase transfer of carbon dots between an organic phase and aqueous solution triggered by CO₂. *Angew. Chem. Int. Ed.* **2018**, *57*, 3687–3691. [[CrossRef](#)] [[PubMed](#)]
42. Surendran, P.; Lakshmanan, A.; Vinitha, G.; Ramalingam, G.; Rameshkumar, P. Facile preparation of high fluorescent carbon quantum dots from orange waste peels for nonlinear optical applications. *Luminescence* **2020**, *35*, 196–202. [[CrossRef](#)] [[PubMed](#)]
43. Capisciano, V.; Giacalone, F.; Gruttadauria, M. Is a Catalyst Always Needed? The Case of the Knoevenagel Reaction with Malononitrile. *ChemCatChem* **2022**, *14*, e202200696. [[CrossRef](#)]
44. Ma, X.; Li, X.; Zhou, J.; Wang, Y.; Lang, X. Anchoring dye onto 1D Nb₂O₅ in cooperation with TEMPO for the selective photocatalytic aerobic oxidation of amines. *Chem. Eng. J.* **2021**, *426*, 131418. [[CrossRef](#)]

45. Ito, T.; Seidel, F.W.; Jin, X.; Nozaki, K. TEMPO as a hydrogen atom transfer catalyst for aerobic dehydrogenation of activated alkanes to alkenes. *J. Org. Chem.* **2022**, *87*, 12733–12740. [[CrossRef](#)] [[PubMed](#)]
46. Hayyan, M.; Hashim, M.A.; AlNashef, I.M. Superoxide ion: Generation and chemical implications. *Chem. Rev.* **2016**, *116*, 3029–3085. [[CrossRef](#)]
47. Gajaganti, S.; Bajpai, S.; Srivastava, V.; Singh, S. An efficient, room temperature, oxygen radical anion ($O_2^{\bullet-}$) mediated, one-pot, and multicomponent synthesis of spirooxindoles. *Can. J. Chem.* **2017**, *95*, 1296–1302. [[CrossRef](#)]
48. Hojatti, M.; Kresge, A.J.; Wang, W.H. Cyanocarbon acid. Direct evidence that their ionization is not an encounter-controlled process and rationalization of the unusual solvent isotope effects. *J. Am. Chem. Soc.* **1987**, *109*, 4023–4028. [[CrossRef](#)]
49. Zhang, X.M.; Yang, D.L.; Liu, Y.C.; Chen, W.; Cheng, J.L. Kinetics and mechanism of the reactions of o- and p-nitrohalobenzenes with the sodium salt of ethyl cyanoacetate carbanion: A non-chain radical nucleophilic substitution mechanism. *Res. Chem. Intermed.* **1989**, *11*, 281–300. [[CrossRef](#)]
50. Roschangar, F.; Sheldon, R.A.; Senanayake, C.H. Overcoming barriers to green chemistry in the pharmaceutical industry—the Green Aspiration Level™ concept. *Green Chem.* **2015**, *17*, 752–768. [[CrossRef](#)]
51. Michenzi, C.; Proietti, A.; Rossi, M.; Espro, C.; Bressi, V.; Vetica, F.; Simonis, B.; Chiarotto, I. Carbon nanodots from orange peel waste as fluorescent probes for detecting nitrobenzene. *RSC Sustain.* **2024**, *2*, 933–942. [[CrossRef](#)]
52. Naskar, K.; Maity, S.; Maity, H.S.; Sinha, C.K. A reusable efficient green catalyst of 2D Cu-MOF for the click and Knoevenagel reaction. *Molecules* **2021**, *26*, 5296. [[CrossRef](#)] [[PubMed](#)]
53. Kalar, P.L.; Jain, K.; Agrawal, S.; Khan, S.; Vishwakarma, R.; Shivhare, A.; Deshmukh, M.M.; Das, K. Green synthesis of electrophilic alkenes using a magnesium catalyst under aqueous conditions and mechanistic insights by density functional theory. *J. Org. Chem.* **2023**, *88*, 16829–16844. [[CrossRef](#)] [[PubMed](#)]
54. Khan, D.; Mukhtar, S.; Alsharif, M.A.; Alahmadi, M.I.; Ahmed, N. $PhI(OAc)_2$ mediated an efficient Knoevenagel reaction and their synthetic application for coumarin derivatives. *Tetrahedron Lett.* **2017**, *58*, 3183–3187. [[CrossRef](#)]
55. Meng, G.; Gao, S.; Liu, Y.; Zhang, L.; Song, C.; Huang, K. Amino- and sulfo-bifunctionalized hyper-crosslinked organic nanotube frameworks as efficient catalysts for one-pot cascade reactions. *New J. Chem.* **2019**, *43*, 2269–2273. [[CrossRef](#)]
56. Jain, K.; Chaudhuri, S.; Pal, K.; Das, K. The Knoevenagel condensation using quinine as an organocatalyst under solvent-free conditions. *New J. Chem.* **2019**, *43*, 1299–1304. [[CrossRef](#)]
57. Nicholson, W.; Howard, J.; Magri, G.; Seastram, A.; Khan, A.; Morrill, L.C.; Richards, E.; Browne, D. Ball-milling-enabled reactivity of manganese metal. *Angew. Chem. Int. Ed.* **2021**, *60*, 23128–23133. [[CrossRef](#)]
58. Wu, D.P.; Ou, W.; Huang, P.Q. Ir-catalyzed chemoselective reductive condensation reactions of tertiary amides with active methylene compounds. *Org. Lett.* **2022**, *24*, 5366–5371. [[CrossRef](#)]
59. Javad Kalbasi, R.; Khojastegi, A. Hierarchically pore structure poly 2-(dimethyl amino) ethyl methacrylate/Hi-ZSM-5: A novel acid–base Bi-functional catalyst as heterogeneous platform for a tandem reaction. *Catalysis Lett.* **2018**, *148*, 958–971. [[CrossRef](#)]
60. Yamakoshi, H.; Shibata, D.; Bando, K.; Kajimoto, S.; Kohyama, A.; Egoshi, S.; Dodo, K.; Iwabuchi, Y.; Sodeoka, M.; Fujita, K.; et al. Ratiometric analysis of reversible thia-Michael reactions using nitrile-tagged molecules by Raman microscopy. *Chem. Commun.* **2023**, *59*, 14563–14566. [[CrossRef](#)]
61. Vilela, G.G.; dos Santos Silva, W.F.; de Melo Batista, V.; Rocha Silva, L.; Maus, H.; Hammerschmidt, S.J.; Crisóstomo Bezerra Costa, C.A.; da Silva Moura, O.F.; Duarte de Freitas, J.; Lobo Coelho, G.; et al. Fragment-based design of α -cyanoacrylates and α -cyanoacrylamides targeting Dengue and Zika NS₂B/NS₃ proteases. *New J. Chem.* **2022**, *46*, 20322–20346. [[CrossRef](#)]
62. Krech, A.; Yakimchyk, V.; Jarg, T.; Kananovich, D.; Ošek, M. Ring-opening coupling reaction of cyclopropanols with electrophilic alkenes enabled by decatungstate as photoredox catalyst. *Adv. Synth. Catal.* **2024**, *366*, 91–100. [[CrossRef](#)]
63. Hayashi, Y.; Han, X.; Mori, N. Secondary amine-mediated domino reaction for the synthesis of substituted quinolines from dicyanoalkenes and enynals. *Chem. Eur. J.* **2023**, *29*, e202301093. [[CrossRef](#)] [[PubMed](#)]

Disclaimer/Publisher's Note: The statements, opinions and data contained in all publications are solely those of the individual author(s) and contributor(s) and not of MDPI and/or the editor(s). MDPI and/or the editor(s) disclaim responsibility for any injury to people or property resulting from any ideas, methods, instructions or products referred to in the content.